ISBN: 978-3-95450-132-8 doi:10.18429/JACoW-IPAC2014-TUPRO098

DESIGN AND TEST OF DIPOLE AND QUADRUPOLE MAGNETS FOR PAL-XFEL*

Hyung Suck Suh#, Bongi Oh, Dong Eon Kim, Heung-Sik Kang, Hong-Gi Lee, In Soo Ko, Ki-Hyeon Park, Moo Hyun Cho, Sang-Bong Lee, Young-Gyu Jung
PAL, Pohang, Republic of Korea

Abstract

PAL-XFEL, currently under construction in Pohang, Korea, will consist of a 10 GeV linac, three hard X-ray branches and two soft X-ray branches. As the first phase of this project, one hard X-ray and one soft X-ray branches will be constructed. This facility requires 7 different families of dipole magnets, and 11 families of quadrupole magnets. We have designed these magnets with the water cooling or the heat sink system. In this presentation, we describe the modified design of the magnets for the efficient manufacture, and the magnetic and thermal analysis with the test results.

INTRODUCTION

The PAL (Pohang Accelerator Laboratory)-XFEL is a 0.1-nm hard X-ray FEL project starting from 2011. Three hard X-ray and two soft X-ray branches will be planned. As the first phase of this project, one hard X-ray (HX1) and one soft X-ray (SX1) will be constructed [1]. We have designed all magnets on our own by using OPERA and ANSYS codes [2, 3]. In the process of the design, it was helpful to parameterize the main figures of the magnets in a spread sheet for easy estimation by one parameter change. Now we are manufacturing them and tested the first prototype magnets.

DIPOLE MAGNETS

The dipole magnets were classified into 7 kinds according to the pole gap, the effective magnetic length, and the maximum magnetic field. The results of the classification are listed in Table 1. Most dipole magnets have the same pole gaps of 30 mm except D6 for the self-seeding. D3 and D7 for the dump dipole magnets have C-type core shape, and the rest of all have H-type which has good symmetry.

Table 1: The Families of Dipole Magnets

Family	Magnetic length [m]	Max. field [T]	Trim coil	Qty
D1	0.20	0.80	yes	6
D2	0.60	1.00	yes	18
D3	1.50	1.30	yes	11
D4	0.17	0.30	yes	4
D5	0.40	1.20	yes	1
D6	0.40	0.262	yes	4
D7	0.75	1.164	no	2

*Work supported by Ministry of Science, ICT and Future Planning of Korea, #suhhs@postech.ac.kr

The maximum temperature rise of all coils is estimated less than 15 K for the stable operation, but the numbers of cooling circuit per magnet vary 2~6 as magnet families. All dipole magnets of D1~D6 for the bunch compressor, the chicane, and the self-seeding have the trim coil with 1% magnetic field of the main field.

The pole profiles of magnets are optimized by the small bumps at the tip of the pole for the field uniformity. The requirements for the field uniformity are different from each magnet, e.g. in the case of H-type dipole magnet D1, $\Delta B/B_0 < 1.0E\text{-}4$ for ±17mm, 5.0E-4 for ±41mm in 3D calculation. So the pole contour of D1 is made like Fig. 1 where the a-b line has a slight slope. The 2D/ 3D field uniformities of are shown in Fig. 2.

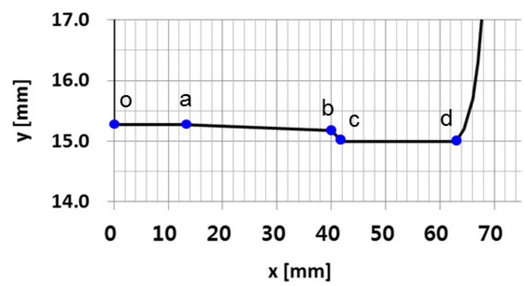

Figure 1: Pole contour of H-type dipole magnet D1.

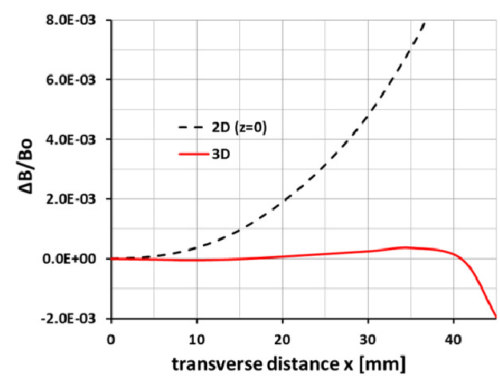

Figure 2: 2D/3D field uniformities of dipole magnet D1.

The laminated cores are used for the magnets D2 and D3 which quantities are more than 10 magnets, and the solid cores are used for the rest of the dipole magnets.

We measured the magnetic field of the dipole magnet D4 that have four coils per magnet for the space in the middle (see Fig. 3). The 3D results of the field uniformity satisfied the requirement that is less than 1.0E-4 within ±9 mm as shown Fig. 4, and the temperature rise was 6 K on the surface of coil similar to the estimate of 8 K [4].

ISBN: 978-3-95450-132-8 doi:10.18429/JACoW-IPAC2014-TUPRO098

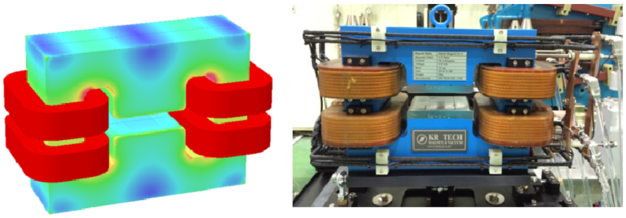

Figure 3: The FEM model and the prototype of dipole magnet D4.

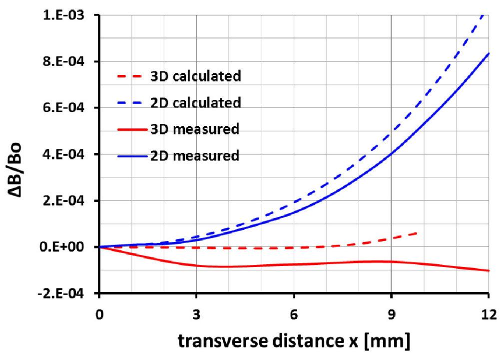

Figure 4: Field deviation comparison of dipole magnet D4.

QUADRUPOLE MAGNETS

The quadrupole magnets are classified into 11 kinds according to the aperture diameter, the effective length, and the maximum gradient. The results of the classification are listed in Table 2. We tried to reduce the number of coil types and the number of the power supply types for the convenient manufacture.

There are the horizontal and vertical steering functions in some quadrupole magnets (Q1, Q2, Q3, Q6, and Q9) for the bunch compressors and the inter-undulator.

Table 2: The Families of Quadrupole Magnets

Family	Aperture diameter [mm]	Magnetic length [m]	Max. gradient [T/m]	Qty
Q1	30	0.065	15	21
Q2	30	0.13	25	64
Q3	30	0.18	25	17
Q4	44	0.20	25	10
Q5	22	0.40	35	14
Q6	16	0.13	40	31
Q7	80	0.50	18	3
Q8	22	0.25	30	15
Q9	16	0.08	32	18
Q10	44	0.50	25	4
Q11	44	0.10	10	12

The multipole components were calculated by using an equation, the radial component: $B_r(r_0,\varphi) = \Sigma_n \{A_n \sin(n\varphi) + B_n \cos(n\varphi)\}$, where r_0 is the reference radius that is the good field radius. All magnets are optimized to have the relative multipole components less than 1.0E-4 in 3D calculations. Figure 5 shows the half pole contour. In this figure the o-m line follows along a hyperbola, the m-n is a straight and an arc after n point. We could satisfy the multipole requirements by manipulating the position and the length of the straight section.

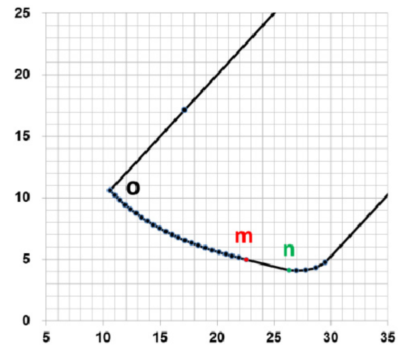

Figure 5: The half pole of quadrupole magnet.

The indirect cooling system (heat sink) for the quadrupole magnets (Q1, Q2, Q3, Q5, Q6, Q8, and Q9) was adopted. Figure 7 shows the cross section of the conductor and the temperature distribution of quadrupole magnet Q2. We used the effective thermal conductivity: $1/k_{eff} = \Sigma v_i/k_i$ for the turn insulation and the ground insulation, where v_i is the volume fraction.

We made a prototype quadrupole magnet Q2, and measured the magnetic field with a hall probe and the temperature rise on June 2014 (see Fig. 6). The relative deviation of the field gradient ΔB'/B' was shown as 1.2E-3 within ±10mm on the mid-plane.

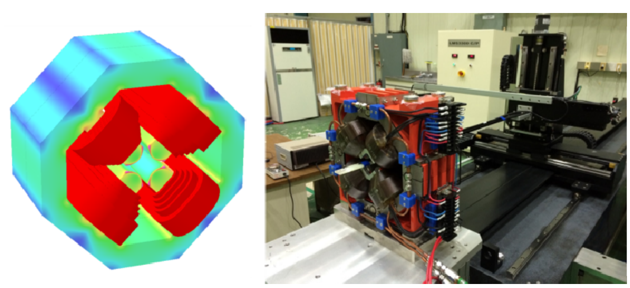

Figure 6: FEM model and field measurement scene of a quadrupole magnet Q2.

The measured temperature rise is 14 K on the surface of conductor and is 16 K by calculating the coil resistance, but the maximum estimate was 11 K in conductor as shown in Fig. 7. There is some discrepancy.

We prepare the field clamp to shield the leakage field from quadrupole magnets. The field clamp of 1 mm thickness can reduce the leakage field to less than 5 Gauss behind this clamp. This field clamp reduces the magnetic length by about 1% for Q2.

ISBN: 978-3-95450-132-8 doi:10.18429/JACoW-IPAC2014-TUPRO098

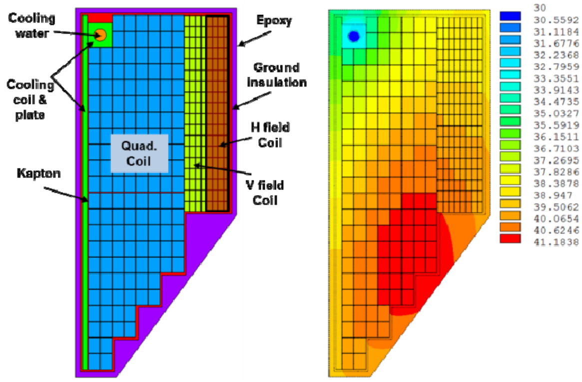

Figure 7: The conductor cross section and the temperature distribution of quadrupole magnet Q2 with a heat sink.

CORRECTOR MAGNETS

The dipole magnets and the quadrupole magnets for the chicanes and the beam analysing have the trim coils or the horizontal/vertical steering coils respectively. Beside from these, we prepare the independent correctors of 43 that are composed of 36 with iron core and 14 with air core. Other correctors with iron core have the heat sink system similar to Fig. 7 for the narrow space. The main parameters of the corrector magnets are shown in Table 3.

Table 3: The Main Parameters of Corrector Magnets

Corrector type	Iron core (air)	Iron core	(Fast) corrector
Core	iron	iron	air
Cooling type	air	heat sink	air
Field integral [Gcm]	5000	5000	1000
Magnet length [mm]	295	144	200
Current density [A/mm^2]	1.1	2.6	1.2
Temperature rise, h=10 [K]	19	10	21
Quantity	36	6	14

h: convection coefficient

CONCLUSION

When we classify the magnets and choose the coil sizes we should consider the electrical properties of magnets, the connection condition of magnets in series or stand alone, and the number of cooling circuit. If we increase the number of cooling circuit in order to reduce the temperature rise, then the magnets become more complicate with the risk of leakage.

We have designed almost all magnets, and are testing the prototype magnets now. The results of tests are not bad until now. But we have to modify magnets if it is necessary after strict analyses of the magnetic field and the temperature rise.

REFERENCES

[1] PAL-XFEL, Beam Optics and Parameter Design, Heung-Sik Kang, 2012.
[2] Vector Fields Software, http://www.cobham.com
[3] ANSYS, http://www.ansys.com
[4] “Iron Dominated Electromagnets”, Jack T. Tanabe, 2005.